Excitation of the giant resonance region in silicon by inelastic scattering of 115 MeV protons

S. Kailas,* P. P. Singh, A. D. Bacher, C. C. Foster, D. L. Friesel, P. Schwandt, and J. Wiggins
Indiana University Cyclotron Facility, Bloomington, Indiana 47405
(Received 27 October 1981)

Differential cross sections for the excitation of the giant resonance region in silicon have been measured over the angular range 10° to 34° by inelastic scattering of 115 MeV protons. The giant resonance exhibits fine structure which is similar to that observed in (α,α') and low-energy (p,p') data. The angular distribution for the giant resonance has been analyzed in terms of the distorted-wave Born approximation and 19–26% of the energy weighted sum rule strength for $L=2$ has been identified. It is also found that the angular distribution for the excitation of the giant resonance region cannot be explained by assuming only the presence of giant quadrupole resonance.

[NUCLEAR REACTIONS Si(p,p'), $E=115$ MeV; measured $\sigma(\theta)$ for giant-resonance excitations and the low lying levels. Calculated energy-weighted sum rule strengths.]

I. INTRODUCTION

The existence of isoscalar giant resonances (GR), in particular the giant quadrupole resonance (GQR) (Refs. 1 and 2) and the giant monopole resonance (GMR) (Ref. 3) has been well established, primarily by experiments involving the inelastic scattering of alpha particles. It is of interest to further study the excitation of the GR region with a variety of projectiles at different energies in order to better understand the excitation mechanism of these known structures and also to investigate the strengths of other multipoles. In studies involving light nuclei[4–6] like Mg and Si, the fine structures excited in the GR region using alpha particles and protons have been found to be remarkably similar. This is an interesting result since protons are expected to excite both the isoscalar and isovector components of the GR region while alpha particles excite mainly the isoscalar components.

A detailed study involving the inelastic scattering of alpha particles on Si [Refs. 4(a) and 6] has established that the fine structure in the GR is predominantly quadrupole in nature. The situation for protons is not as well understood. One analysis[1] of proton inelastic scattering measurements at 60 MeV concluded that the observed structures were mainly of dipole character (GDR) with up to 15% of EWSR strength for GQR being excited, depending on the model used for GDR calculation. Furthermore, there has been some uncertainty in calculating the GDR cross section due to the lack of a reliable isovector potential. However, van der Borg *et al.*[4(b)] have recently analyzed the (p,p') data[1] using more reliable isovector potentials due to Patterson *et al.*,[7] and have shown that the GDR is in fact weakly excited and the structures are mainly due to the GQR, in accord with the alpha-particle results. It seems useful to explore this situation at higher proton energies with (p,p') data of quality comparable to that of the (α,α') experiment[4(a)] performed at $E_\alpha=120$ MeV. As the probability of exciting higher order multipoles increases with increasing proton energy, it may also be possible to use higher energy inelastic proton scattering to detect the presence of higher multipoles[8] and perhaps to determine their strengths. Since the earlier low-energy proton results consisted of only three data points defining the angular distribution, it seemed useful to measure the data over a larger angular range. In the present work, we report differential cross section angular distributions for the GR region in silicon by inelastic scattering of 115 MeV protons. Besides the work of van der Borg *et al.*,[6] the GR region in silicon has also been studied by Knopfle *et al.*[9] and Youngblood *et al.*[10] using, respectively, 150 and 126 MeV alpha particles, by Pitthan *et al.*[11] using 91 MeV electrons, and by Bertrand *et al.*[1] using 61 MeV protons.

II. EXPERIMENTAL DETAILS

The present work employed a 115 MeV proton beam from the Indiana University Cyclotron Facility. The scattered particles were detected using two high-purity Ge detectors of thickness 1.5 cm each in a standard ΔE-E counter-telescope configuration. Natural Si (92.21% ^{28}Si) targets of thickness 6.7 and 12.6 mg/cm^2 were used and an overall resolution of better than 250 keV FWHM was obtained. The measurements covered an angular range from 10° to 34°, in 2° steps, with an angular resolution of ±0.5°. Care was taken to minimize beam "halo" problems by fine tuning of the beam and by periodic checking of background with the target replaced by an equivalent empty target frame. A typical energy spectrum obtained for the Si target is shown in Fig. 1. The fine structure in the GR region between 15 and 24 MeV of excitation are clearly evident. The cross sections for various states were calculated after taking into account the target thickness, the incident number of protons, the solid angle of the detector telescope, correction for dead times, and a correction for reaction losses[12] in the Ge detectors. The reaction loss correction amounted to an upward normalization of all cross sections by a factor of 1.1. The error on this correction factor is estimated to be about 15% of the correction.

III. ANALYSIS AND DISCUSSIONS

Cross sections for the well-known low-lying states of ^{28}Si were analyzed in terms of the standard DWBA using the computer code DWUCK4 (Ref. 13) employing collective form factors with complex coupling. The distorted waves were computed using the proton optical model parameters of Nadasen *et al.*[14] who had analyzed the elastic proton scattering in the energy range 80 to 180 MeV for several targets including Si. The parameters used in this study are the following:

$$V_r = -22.75 \text{ MeV}, \quad r_R = 1.265 \text{ fm}, \quad a_R = 0.749 \text{ fm},$$

$$V_I = -6 \text{ MeV}, \quad r_I = 1.409 \text{ fm}, \quad a_I = 0.644 \text{ fm},$$

$$V_{so} = -3.43 \text{ MeV}, \quad W_{so} = 1.38 \text{ MeV},$$

$$r_{so} = 0.972 \text{ fm}, \quad a_{so} = 0.588 \text{ fm}, \quad r_{Coul} = r_R .$$

In Fig. 2 we compare experimental differential cross sections for the low-lying states with the

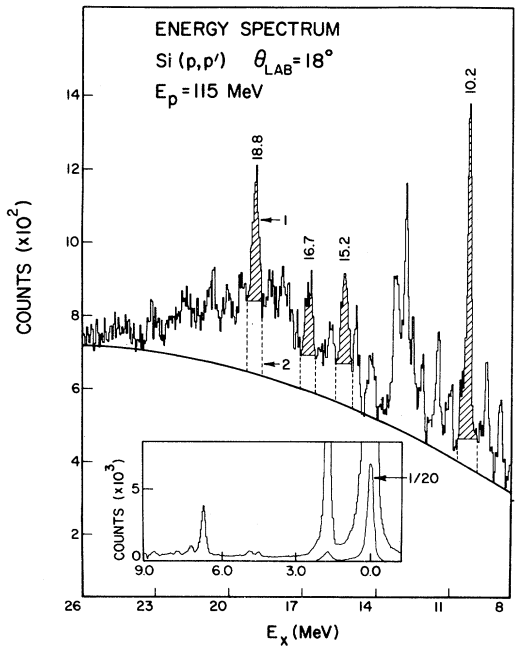

FIG. 1. Energy spectrum in the GR region for inelastic proton scattering from Si. The assumed underlying continuum is indicated by the smooth curve. The excitation region covering the ground state and low-lying states in ^{28}Si is shown as an insert.

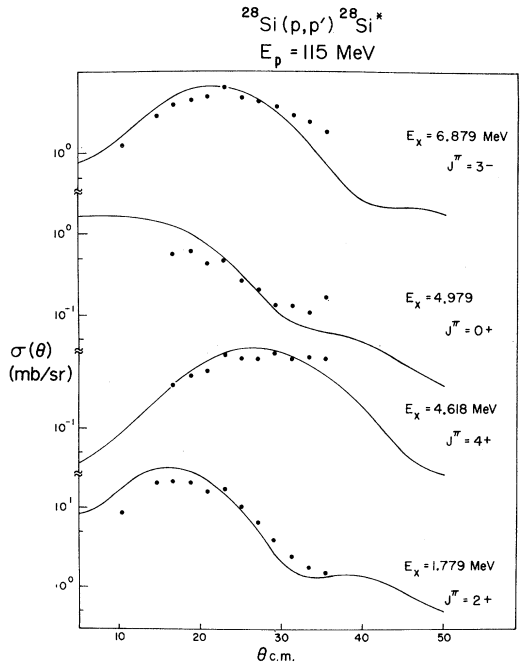

FIG. 2. Measured angular distribution (dots) for the low-lying levels of ^{28}Si compared with DWBA predictions (curves).

DWBA predictions. The agreement between the two is acceptably good. Various energy-weighted sum rule (EWSR) strengths S and transition rates G for these states, calculated by using the procedure of Ref. 15, are listed in Table I along with electromagnetic transition rates $G_{\rm em}$ obtained from the measured lifetimes or inelastic electron scattering wherever available.[15(a)] The EWSR strengths are calculated using both a uniform mass distribution with $R=1.2\,A^{1/3}$ fm, (S_U), and a Fermi mass distribution (S_F). As is apparent from Table I the values of S_U and S_F differ significantly; in general, S_U is somewhat larger than S_F. As also found in the (α,α') analysis,[4(a)] the transition rates obtained from the DWBA analysis of the (p,p') data do not agree with the electromagnetic $G_{\rm em}$ values. These differences have been attributed[15,15(b),15(c)] to dissimilarities in radial behaviors of the exact hadronic transition operator and the "equivalent electromagnetic" transition operator used in the conventional DWBA calculations. These differences are expected[15,15(c)] to increase with projectile energy because the exact transition operator samples more and more of the interior of the transition density whereas the "equivalent electromagnetic" operator is always more sensitive to the tail of the transition density. At very low energies, due to stronger absorption, both procedures lead to similar results for transition rates. Furthermore, because of the complicated structure of the exact hadronic transition operator[15(c)] these differences may also depend upon the Q value and the L transfer. In light of these difficulties, ideally one ought to employ microscopic calculations with realistic hadronic transition operators. While progress is being made towards this end, most present analyses of inelastic cross sections to obtain transition rates or EWSR strength are performed in terms of the collective model DWBA. A phenomenological correction for the effects mentioned above is incorporated by normalizing the DWBA values of the transition rates, $G_{\rm DWBA}$, to the $G_{\rm em}$ for states of given J, where known, and the empirically normalizing by the same factor the $G_{\rm DWBA}$ for other cases of the same J. Although we recognize possible pitfalls in this procedure, it is in this spirit that the results of the DWBA analysis for higher excitation states are carried out in this paper. Since experience[15,15(c)] has shown that using Fermi mass distributions and "complex coupling" in the DWBA calculations leads to smaller values for the normalization, the discussion here is restricted to these choices. In column nine of Table I, $N(\equiv G_{\rm em}/G_F)$ represents the normalization referred to above and the S_n are the normalized EWSR strengths for various low-lying states. For comparison, values of N obtained in the collective model DWBA analysis of the ^{28}Si$(\alpha,\alpha')^{28}$Si data at 120 MeV are also given. While values of this empirical normalization constant as obtained from the analysis of the (p,p') data are different from those obtained[4(a)] for (α,α') data, the relative dependence of N on the L (J) transfer is similar. Although ^{28}Si$(p,p')^{28}$Si* data for the low-lying states exist in the literature at proton energies of 100 MeV,[16] 155 MeV,[17] and 185 MeV,[18] up to now no extensive DWBA calculations have been reported. It will be interesting to carry out these analyses and study the energy dependence of the empir-

TABLE I. Isoscalar transition rates and EWSR strengths obtained for low lying states.

E_x (MeV)	J^π	βR (fm)	S_U[a] (%)	G_F[b] (W.u.)	S_F[a] (%)	$G_{\rm em}$[b] (W.u.)	S_n[d] (%)	N[c]	N_α[e]
1.78	2^+	1.70	16.6	21.1	15.5	12.6	9.3±3.2	0.60	1.11
4.62	4^+	0.49	1.0	4.4	0.55	7.4	0.9±0.3	1.70	3.93
6.89	3^-	1.02	11.0	11.1	8.5	12.3	9.4±3.1	1.11	2.28
4.98	0^+	0.35	4.0		6.8		4.2±2.1	0.62[f]	0.66[f]

[a] S_U and S_F stand for energy weighted sum rule (EWSR) values obtained using uniform and Fermi mass distributions.

[b] G_F stands for the transition rate using a Fermi distribution whereas $G_{\rm em}$ represents transition rates obtained from the measured life times for the states as quoted in Ref. 15(a).

[c] Normalization constant $N=G_{\rm em}/G_F$.

[d] S_n are normalized EWSR values, i.e., $S_n=NS_F$.

[e] N_α represents normalization constants obtained from the DWBA analysis of ^{28}Si$(\alpha\alpha')^{28}$Si*.

[f] This normalization constant represents the ratio $S_{\rm em}/S_F$, with $S_{\rm em}$ obtained from the work of Strehl (Ref. 27).

ical normalization constant.

One of the problems in the determination of GR yields has been the proper estimation of the nuclear continuum (labeled "background") underlying the fine structures of GR region. This background is expected to arise from a combination of preequilibrium, knockout, and multistep processes and inelastic excitation of continuum states. Since no reliable theory exists to calculate the magnitude and shape of the continuum, we have followed the procedure conventionally employed in previous GR work and treat the continuum as a background of empirically-determined shape. In the present work we have used a second-order polynomial in energy to describe the background shape. Figure 1 illustrates a typical background shape employed in the present analysis. The principal contribution to the error in determining the GR cross section comes from the uncertainty in the procedure for parametrizing the background. In the present analysis, we estimate that the internal consistency in establishing the background contribution leads to an overall error that increases from 15–20% in the angular range 10°–28° to 25–30% for angles greater than 28°. The statistical error in the estimation of GR yields was better than 1% for the entire angular range covered in this study and hence has a negligible contribution to the total error.

In the literature, three different excitation energy (E_x) regions have been used to define the GR region in the case of a Si target. The E_x regions used are 15.9–22.8 MeV, 16.9–24.8 MeV, and 17–22 MeV in Refs. 6, 9, and 1, respectively. We have computed the cross sections for each of the above mentioned regions as well as for the E_x range 15.7–24.1 MeV. This was done to see how the relative strengths of the various multipoles change with different E_x ranges.

The observed angular distribution for the 15.7–24.1 MeV excitation of the giant resonance region is shown in Fig. 3. Its shape does not correspond to that observed for the low-lying states of specific J^π (see Fig. 2) or to the predictions (see Fig. 3) of DWBA for various L transfers at the mean energy of excitation. This confirms the prevailing view that the giant resonance region has contributions from a variety of multipolarities. In performing the DWBA calculations for $L=2$, 3, and 4 we used the conventional collective[19] form factors but for $L=0$ (GMR) and $L=1$ (GDR) we used the prescription due to Satchler.[19] For the GDR we performed calculations using both the phenomenological energy-dependent isovector potential $V_{\rm sym}$, determined by Kwiatkowski and Wall[20] and that calculated from the Bruekner Hartree Fock model of Jeukenne *et al.*[21] The strength and shape parameters used are given below.

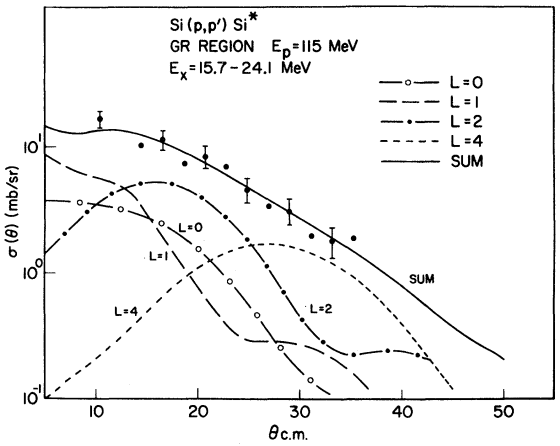

FIG. 3 Differential cross section versus the center of the mass scattering angle for the GR excited in the region $E_x=15.7-24.1$ MeV. The individual contributions of $L=0$, 1, 2, and 4, as well as their sum, which gives the best overall account of the observed angular distribution, are shown as curves. The error due to continuum subtraction procedure varies from 15–30% over this angular range. The error bars shown for a few representative points reflect this uncertainty. Statistical errors are less than 1%.

Jeukenne et al. $V_R=1.90$ MeV; $V_I=10.14$ MeV; $r_R=0.956$ fm; $r_I=1.013$ fm; $a_R=0.774$ fm; $a_I=0.783$ fm; $V_R'=2.81$ MeV; $V_I'=2.14$ MeV; $Vf(x)-V'[df(x)]/dx$.

Kwaitkowski and Wall. $V_{\rm sym}=31.2$ MeV$-0.12E$ (MeV); $r_R=1.22$ fm; $a_R=0.795$ fm. Woods-Saxon form: $f(x)=[1+\exp(x)]^{-1}$; $x=(r-R)/a$; $R=rA^{1/3}$.

The GDR cross section obtained using the latter prescription was found to be ~25% of that obtained using the phenomenological potential. In the following, GDR cross sections were calculated using the phenomenological isovector potential and Goldhaber-Teller (GT) form factors as compared to Jenson-Steinwedel form factor. The former is expected to be the dominant mode for exciting GDR in light nuclei.[22]

In order to extract the contributions of various multipolarities in the GR region the observed angular distribution was fitted by a nonlinear least-squares technique using the predicted angular distribution for $L=0$ to 4 as described above. In this analysis the contribution of the GDR was kept

fixed to the value predicted by the GT model normalized to $E1$ strength as observed from photonuclear measurements. We have assumed that 60% of the EWSR for GDR is located in the excitation region of 15.7—24.1 MeV; this is an average of the 50% to 70% of EWSR strength reported to have been observed for GDR in photonuclear measurements.[23(a),23(b)] The solid curve in Fig. 3 represents the summed contribution of all multipolarities. In Table II we list the transition rates and/or EWSR strengths of various multipolarities for the 15.7 to 24.1 MeV excitation region obtained in this manner. The transition rates for different L values have been corrected by the normalization constants obtained from the analysis of the low-lying states of corresponding J^π. In Table II we also list the values of EWSR strengths for various multipolarities as obtained in other measurements.

The normalized quadrupole strength in the giant resonance region agrees well with that obtained in (α,α') and (e,e') (Ref. 11) measurements. This establishes confidence in the procedure used to analyze the observed angular distributions and in the normalization procedure used to obtain the various strengths. The fact that smaller GQR strength is seen in (α,γ) studies[24] is not surprising since it corresponds to that part of the GQR strength which decays to the ground state of ^{24}Mg.

The amount of $L=4$ strength observed in the GR is consistent with that predicted by theoretical calculations[8] for this mass region. It should be emphasized that the strength assigned to $L=4$ excitation is very much dependent on the cross sections extracted for angles beyond 24° where the procedure for determining the background has larger uncertainties. The $L=3$ strength extracted from the present work should only be looked upon as an upper limit. The accuracy with which the GMR strength can be extracted is not very high (see summary section for additional discussion).

Recently, Schmid[25] reported a fully microscopic calculation of the structure of the giant multipole resonances in ^{28}Si employing angular momentum projected Hartree-Fock and the particle-hole method. He calculated the electromagnetic ground state transitions of both parities and of various multipolarities using both an oscillator and a Woods-Saxon representation. In Table II we list the sum rule strengths obtained by this microscopic calculation (average of strengths obtained from oscillator and Woods-Saxon representation), and they compare favorably with that extracted from the present

TABLE II. Transition rates and EWSR strengths obtained for the 15.7—24.1 MeV GR region.

J^π	βR (fm)	S_U[a] (%)	S_F[a] (%)	S_n (%)[a] (p,p')	S_n (%)[b] (p,p')	S_n (%)[c] (α,α')	S_n (%)[d] (α,γ)	S_n (%) others
0^+	0.50	32	54	34 $\pm$33		>0, <19		~ 10[h]
1^-				60 (fixed)	40(40)			50[e](70)[f]
2^+	0.72	33	31	19 $\pm$3	30(15)	25^{+9}_{-4}	14.5	14—26[g] ~ 26[h]
3^-	0.24	1.8	1.4	1.5$\pm$ 1.5		$\simeq 3$		~ 8[h]
4^+	0.69	8.4	4.7	8 $\pm$ 2				~ 5[h]

[a]See footnotes for Table I for definitions of these symbols. The errors quoted for S_n values obtained in the present work arise primarily from the uncertainties in the continuum background. See text for the procedures used for background subtraction and the errors introduced by it to the cross sections for GR. Errors in the sum rule values introduced due to statistical uncertainties in the cross sections are comparatively negligible.

[b]From the analysis reported in Ref. 4(b) using data of Ref. 1. Values given in parentheses are those quoted in Ref. 1 (covers an excitation region of 17—22 MeV); (p,p') at $E_p \simeq 61$ MeV.

[c]From Ref. 4(a) (covers an excitation region of 14—25 MeV), (α,α') at $E_\alpha \simeq 120$ MeV.

[d]From Ref. 24; (α,γ) measurement.

[e]From Ref. 23(a); photonuclear reaction; number quoted as read from Fig. 18.

[f]From Ref. 23(b); photonuclear reaction; number quoted as read from Fig. 10.

[g]From Ref. 11; (e,e') at $E_e \simeq 91.2$ MeV.

[h]From Ref. 25; microscopic calculation. Average of strengths obtained from oscillator and Woods-Saxon representation.

and other experiments.

The observed angular distributions for other excitation energy regions that have been used[1,6,9] to delineate the GR in the literature were also analyzed in a similar manner. The relative contribution of various multipolarities is found not to differ significantly for various definitions of the excitation regions.

In Fig. 4 we present the energy spectra in the GR region obtained in (p,p'), (α,α'), and (e,e') studies.[26] While the excitation energies of the fine structures seen with the different probes are remarkably similar, the relative strengths of various peaks vary considerably. In an attempt to understand the character of the individual structures and the distribution of strength of various multipolarities, we have

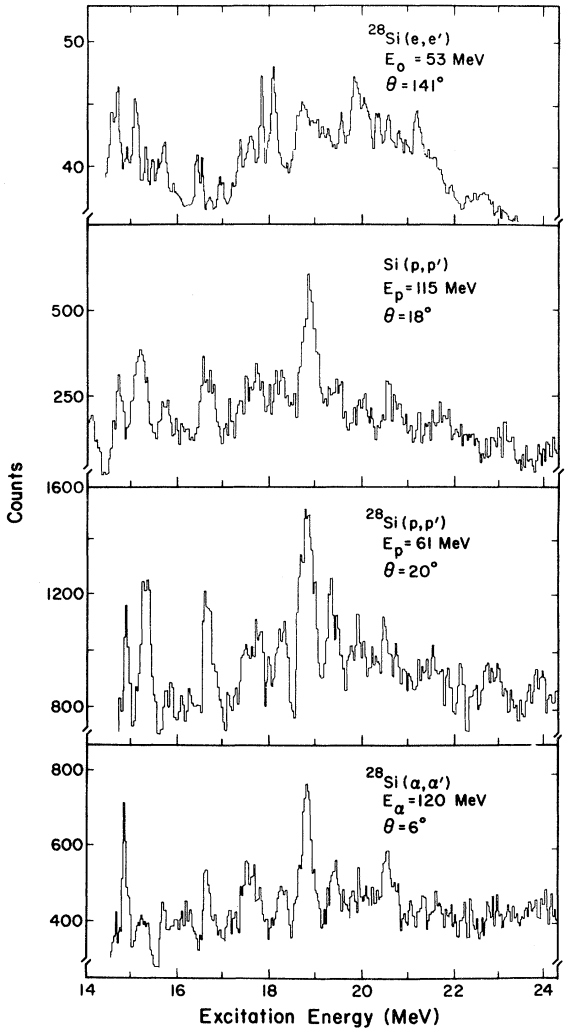

FIG. 4. Comparison of the energy spectra for the GR region obtained from inelastic scattering of electrons, protons, and alphas from Si.

analyzed several of the more prominent peaks separately. The angular distribution of the peaks located at 10.2, 15.2, 16.7, and 18.8 MeV are shown in Fig. 5(a). The yield for these peaks correspond to the shaded region (1) as illustrated in Fig. 1. In Fig. 5(b) are shown the angular distributions of rectangular areas (region 2 in Fig. 1) underneath each of the four peaks but above the continuum background. In part (c) of Fig. 5 are shown the angular distribution of the sum of the two regions. The curves in Fig. 5 represent the predictions of the DWBA calculations. The angular distribution for the 10.2 MeV peak has an almost pure $L=3$ character [see Fig. 5(a)], which is in accord with that found[4(a)] in the (α,α') study. This peak exhausts $\simeq 5\%$ of EWSR strength for $L=3$ as compared to 4.9% found in (α,α') work. The angular distribution of region 2 under this peak reaches a maximum at a slightly larger angle, thus implying a noticeable ($\sim 3\%$ of EWSR) strength for $L=4$. The angular distribution for the 15.2 MeV peak shows the distinctive $L=1$ rise in the forward directions but significant contributions of $L=2$ (1%) and $L=3$ (2%) are required to understand the total yield in this excitation region above the continuum background. This is to be compared with 1% of EWSR found for $L=2$ and 0.4% for $L=3$ found in (α,α') studies[4] for this structure. The angular distribution of the 16.7 MeV peak does not have a clear character as compared to the area beneath it (region 2) which shows forward angle peaking characteristics of $L=1$. On the whole we find about 10% EWSR strength for $L=1$, and 2% for $L=3$ in the combined $(1+2)$ region of this peak. The (α,α') results[4(a)] give $1-1.5\%$ of EWSR for $L=2$ for this region. It is worth pointing here that the structure around 16.7 MeV as seen in (p,p') studies is significantly broader than that seen in (α,α') (see Fig. 4), which may partially explain the difference between the two results. The angular distribution of both the peak at 18.8 MeV and the rectangular area beneath it clearly have contributions from $L=1$ and $L=2$. In total we find 6% of EWSR strength for $L=1$, $\simeq 3\%$ for $L=2$, and $\simeq 2\%$ for $L=3$ in this region. In the (α,α') study[4(a)] $\simeq 4\%$ of EWSR for $L=2$ was found in this energy region. The division into two regions for each peak was made to enhance sensitivity to any multipole character of these structures. Thus, whereas some of the fine structure peaks seen in the GR region may have unique multipolarities, most appear to have a complex character. Furthermore, it appears that different probes may be exciting components of various multipolari-

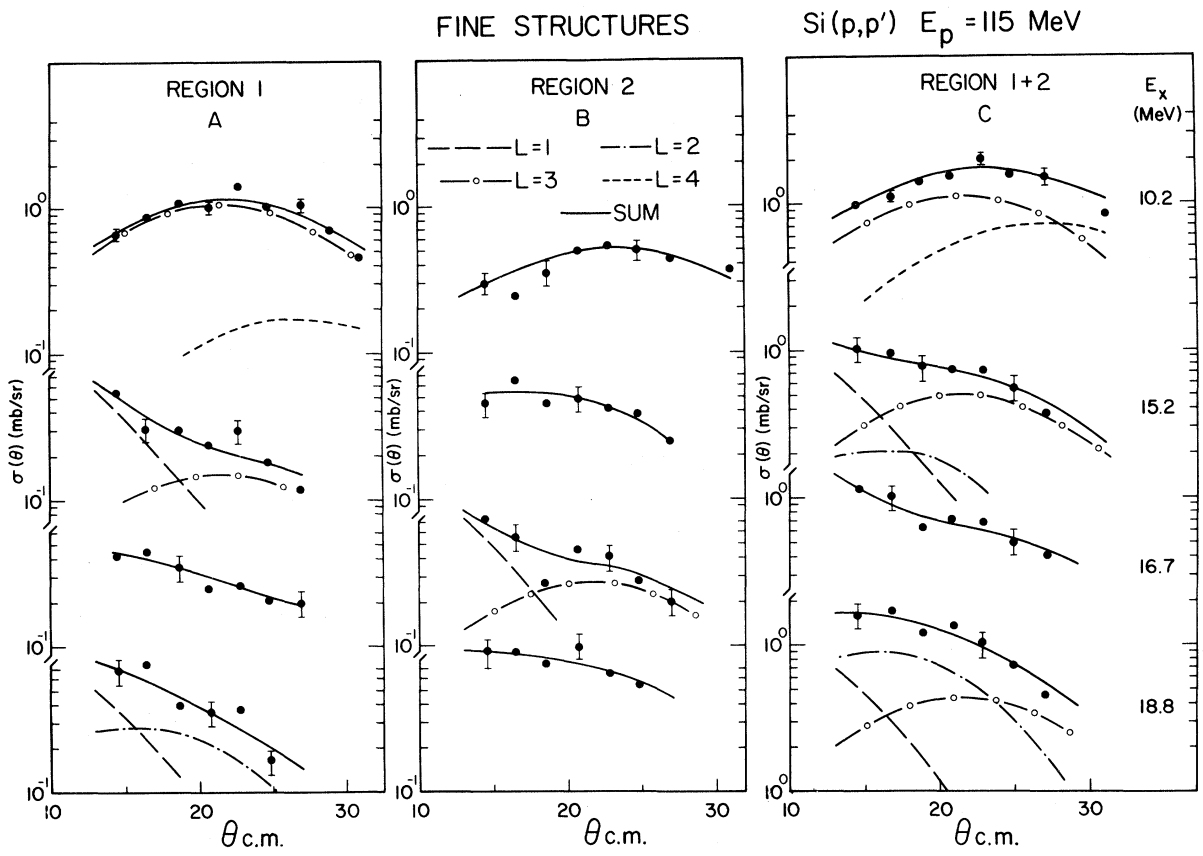

FIG. 5. Angular distributions for the fine structures in the E_x range 9—15 MeV. The curves represent the results of DWBA calculation.

ties in different proportions. This is evident from the observed differences in the relative strengths of different multipolarities and from the unequal widths of structures centered at the same excitation energy. This may account for the observation that the results deduced from the analysis of the (p,p') data do not agree in detail with the (α,α') results for similar regions of excitation, although for the GR region as a whole the two measurements lead to comparable results for EWSR strengths.

IV. SUMMARY

We have reported here measurements of inelastic scattering of 115 MeV protons from a Si target covering the excitation energy range up to ~26 MeV. The cross sections for the low-lying, well-resolved states and those for the giant resonance region have been analyzed in terms of DWBA. The transitions to the low-lying states obtained by DWBA calculations were normalized to the known electromagnetic transition rates for these states. The observed shape of the angular distribution for the giant resonance region is not consistent with dominance of a single multipolarity. By combining DWBA angular distributions for $L=0$ to 4, with weights determined by a nonlinear least square method, EWSR strengths for $L=0$, 2, 3, and 4 multipolarities were determined. After normalizing these with factors obtained for the low lying states we obtained a relatively consistent set of EWSR strengths. Our results indicate that in Si, assuming the presence of 60% EWSR strength for the GDR, 19% of EWSR strength for the GQR lies in the excitation region of 15.7—24.1 MeV excitation and a few percent of the expected EWSR strength for $L=4$. The observed strength for GMR is highly dependent upon the strength assumed for the GDR, the model (GT or JS) used, and the parametrization of the isovector symmetry potential. The value for GMR quoted in Table II is based upon the assumptions outlined above, namely 60% of EWSR strength for the GDR, use of the GT model, and of the phenomenological V_{sym}. Since the angular distibutions for GMR and GDR are forward peaked, the estimate of their strengths is mostly determined by the mea-

sured cross sections at forward angles. For example, the observed cross sections are consistent with zero GMR strength provided the GDR strength is increased to 90% of EWSR. On the other hand, $>30\%$ of the EWSR strength for the GMR is obtained if the GDR contribution is lowered substantially (either by reducing the percentage of EWSR or by reduction in the V_{sym}). The absolute magnitude of the GDR cross sections corresponding to a given fraction of its EWSR strength is also strongly dependent upon the model used. In general, the JS model, for a given V_{sym}, predicts a 2 to 5 times larger GDR cross section per unit strength as compared to the GT model.[4(b)] Thus a significant contribution of the JS-type form factor would result in a lower strength for GMR, if that for GDR is kept fixed at 60% of EWSR as known from the photonuclear results. The effects of variations of the types mentioned above on the strength extracted for higher multipolarity components are progressively smaller since their angular distributions peak successively at larger angles. For example, if the strength of GDR is not constrained, within the framework of the GT model, the data are found to be consistent with (in terms of the EWSR) $\sim 0\%$ of GMR, 90% of GDR, 26% of GQR, and 8% for $L=4$. The extracted strength for $L=2$ and $L=4$ are not changed drastically.

The reservations outlined above notwithstanding, the present work indicates that the presence of GQR alone is not sufficient to explain the angular distribution in the GR region.

It is worth pointing out here that the magnitude of various strengths may be systematically either too high or too low because the electromagnetic transition operator for various multipolarities that is conventionally used in the DWBA analysis is not identical to the hadronic transition operator one should use. It remains to be demonstrated whether the normalization process used here can adequately account for this difference.

The GQR strength observed here is consistent with those obtained in (α,α') and (e,e') studies. Fine structures in the GR region as seen in (e,e'), (p,p'), and (α,α') measurements are similar because they predominantly correspond to GQR excitation which, on an absolute scale, is the dominant excitation mode for all probes.

ACKNOWLEDGMENTS

We wish to thank Dr. M. N. Harakeh, Dr. A. van der Woude, and Dr. A. G. Drentje of K.V.I., Groningen, The Netherlands for useful discussions during their visit to IUCF. This work was supported in part by a grant from the National Science Foundation.

*Permanent address: Bhabha Atomic Research Centre, Bombay, India.

[1]F. E. Bertrand, Annu. Rev. Nucl. Sci. 26, 457 (1976).

[2]G. R. Satchler, Phys. Rev. C 14, 97 (1974).

[3]*Proceedings of the Tropical Conference on Giant Multipole Resonances, Oak Ridge,* edited by F. E. Bertrand (Harwood, New York, 1980).

[4](a) K. van der Borg, K.V.I. Groningen, The Netherlands Ph.D. thesis, 1979. (b) K. van der Borg, M. N. Harakeh, and A. van der Woude, Nucl. Phys. A341, 219 (1980).

[5]F. E. Bertrand, K. van der Borg, A. G. Drentje, M. N. Harakeh, J. van der Plicht, and A. van der Woude, Phys. Rev. Lett. 40, 635 (1978).

[6]K. van der Borg, M. N. Harakeh, S. Y. van der Werf, and A. van der Woude, Phys. Lett. 67B, 405 (1977).

[7]D. M. Patterson, R. R. Doering, and A. Galonsky, Nucl. Phys. A263, 261 (1976).

[8]J. Wamback, F. Osterfeld, J. Speth, and V. A. Madsen, Nucl. Phys. A324, 261 (1979); S. Krewald and J. Speth, Phys. Lett. 52B, 295 (1974).

[9]K. T. Knopfle, G. J. Wanger, A. Kiss, M. Rogge, C. Mayer-Boricke, and T. Bauer, Phys. Lett. 64B, 263 (1976).

[10]D. H. Youngblood, C. M. Rozsa, J. M. Moss, D. E. Brown, and J. D. Bronson, Phys. Rev. C 15, 1644 (1977).

[11]R. Pitthan, F. R. Buskirk, J. N. Dyer, E. E. Hunter, and G. Pozinsky, Phys. Rev. C 19, 299 (1979).

[12]M. Q. Makino, C. N. Waddell, and R. Eisberg, Nucl. Instrum. Methods 60, 109 (1968).

[13]DWUCK4, J. R. Comfort's modified version of original program due to P. D. Kunz.

[14]A. Nadasen, P. Schwandt, P. P. Singh, A. D. Bacher, P. T. Debevec, W. W. Jacobs, M. D. Kaitchuck, and J. T. Meek, Phys. Rev. C 23, 1023 (1981).

[15]A. M. Bernstein, in *Advances in Nuclear Physics,* edited by M. Baranger and E. Vogt (Plenum, New York, 1969), Vol. III, p. 325. (a) P. M. Endt and C. van der Leun, Nucl. Phys. A310, 1 (1978). (b) G. H. Rawitscher and R. A. Spicuzza, Phys. Lett. 37B, 221 (1971). (c) F. Osterfeld, J. Wambach, H. Lenske, and J. Speth, Nucl. Phys. A318, 45 (1979).

[16]Y. S. Horowitz, N. K. Sherman, and R. E. Bell, Nucl.

Phys. A136, 577 (1969).
[17]A. Willis, B. Geoffrion, N. Marty, M. Morlet, C. Rolland, and B. Tatischeff, Nucl. Phys. A112, 417 (1968).
[18]O. Sundberg, A. Johanson, G. Tibell, S. Dahlgren, D. Hasselgren, B. Hoistad, A. Ingmarsson, and P. U. Renberg, Nucl. Phys. A101, 481 (1967).
[19]G. R. Satchler, Nucl. Phys. A192, 1 (1972); A224, 596 (1974); Part. Nucl. 5, 105 (1973).
[20]K. Kwiatkowski and N. S. Wall, Nucl. Phys. A301, 349 (1978).
[21]J. P. Jeukenne, A. Lejeunne, and C. Mahaux, Phys. Rev. C 16, 80 (1977).
[22]W. D. Meyers, W. J. Swiatecki, T. Kodama, L. J. El Javick, and E. R. Hilf, Phys. Rev. C 15, 2032 (1977).
[23](a) J. M. Wyckoff, B. Ziegler, H. W. Koch, and R. Uhlig, Phys. Rev. 137B, 576 (1965). (b) J. Ahrens *et al.*, *Photonuclear Reactions,* edited by E. G. Fuller and E. Hayward (Dowden, Nutchinson, and Ross, Stroudsburg, 1976), p. 405.
[24]L. Meyer-Schutzemeister, R. E. Segel, K. Raghunathan, P. T. Debevec, W. R. Wharton, L. L Ruthledge, and T. R. Ophel, Phys. Rev. C 17, 56 (1978).
[25]K. W. Schmid, Phys. Rev. C 24, 1283 (1981).
[26]The original figure containing the (e,e') low energy $(p,p')^1$ and (α,α') data was provided by Darmstadt group.
[27]P. Strehl, Z. Phys. 234, 416 (1970).